



# GREEN SYNTHESIS OF $\text{CuAl}_2\text{O}_4$ SPINEL NANOPARTICLES USING *JATROPHA CURCAS* LEAF EXTRACT: CRYSTALLOGRAPHIC AND MORPHOLOGICAL INVESTIGATIONS

Kailas A. More<sup>1</sup>, Sampat R. Shingda<sup>2\*</sup>, Pushparaj H. Bhuyar<sup>1</sup>, Parvez S. Ali<sup>3</sup>, Nilesh V. Gandhare<sup>1\*</sup>  
E-mail: [nilkanth81@gmail.com](mailto:nilkanth81@gmail.com), [shingdasampat@gmail.com](mailto:shingdasampat@gmail.com)

<sup>1</sup>Department of Chemistry, Nabira Mahavidyalaya, Katol, RTM Nagpur University, Nagpur, 441302.

<sup>2</sup>Department of Chemistry, Arvindbabu Deshmukh Mahavidyalaya, Barsingi, RTM Nagpur University, Nagpur, 441305.

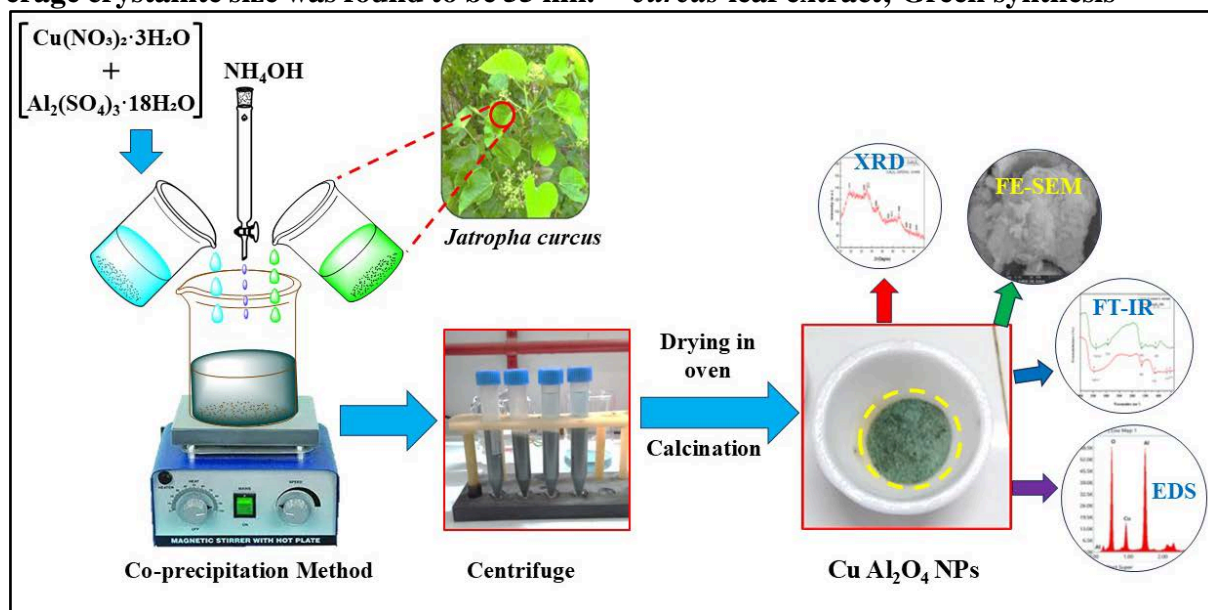
<sup>3</sup>Department of Chemistry, Vidarbha College of Arts, Commerce and Science, Jiwati, Gondwana University, Gadchiroli, 442908-India

## Abstract:

Copper aluminate ( $\text{CuAl}_2\text{O}_4$ ) nanoparticles (NPs) have garnered a lot of interest because of their potential uses in environmental remediation, adsorption, and catalysis. In the current research work,  $\text{CuAl}_2\text{O}_4$  NPs were fabricated using *Jatropha curcas* (*J. curcas*) leaf extract by the co-precipitation method. The Green synthesized  $\text{CuAl}_2\text{O}_4$  nanoparticles were characterized with X-ray diffraction (XRD), which confirmed the spinel structure with a cubic phase, and the average crystallite size was found to be 55 nm.

The chemical as well as structural bonding of  $\text{CuAl}_2\text{O}_4$  NPs and *J. curcas* leaf extract was analyzed by the Fourier-transform infrared spectroscopy (FT-IR) technique. The field-emission scanning electron microscopy (FE-SEM) images show flake-like morphology. The elemental compositions of  $\text{CuAl}_2\text{O}_4$  NPs were determined by energy-dispersive X-ray spectroscopy (EDS) analysis, and equal distribution of elements was confirmed by elemental mapping.

**Keywords:**  $\text{CuAl}_2\text{O}_4$  nanoparticles; *Jatropha curcas* leaf extract; Green synthesis



Graphical Abstract of Green synthesis of  $\text{CuAl}_2\text{O}_4$  Nano particles

## 1. Introduction

The study of spinel synthesis is a fascinating area of inorganic chemistry due to

remarkable structures and potential applications. In the last decade, oxide spinels have seen enormous interest due to their uses in various

fields such as refractories, magnetic materials, pigments, catalysts, optical materials, and electrochemical materials [1-2]. Among the spinel oxides the metal aluminates are valuable material due to their outstanding high mechanical resistance, thermal stability, hydrophobicity, and low surface acidity. Nano structured metal aluminates exhibit enhanced properties such as higher hardness and lower sintering temperatures[3-6]. In the recent years, researchers employed several conventional fabrication techniques including solid state reaction [7], sol-gel [8], wet chemical method [9], chemical co-precipitation [10], microwave [11], solvo thermal [12], hydrothermal [13], polymeric precursor synthesis [14], reverse micelle technique [15], Sono chemical[16] and combustion synthesis [17] have been employed to produce the specific type of spinel aluminates according to the need as per applications. These spinel metal aluminates materials have been significant applications in several industries including ceramics, sensors, and photo catalysis, which are utilized for heat-resistant and the degradation of organic dyes[18-21].

Nowadays, scientists have received a lot of attention on the synthesis of copper aluminate metal oxides due to their intrinsic physical and chemical properties like piezoelectricity, magneto resistance, and superconductivity. Therefore, there is more interest in constructing the spinel  $\text{CuAl}_2\text{O}_4$  NPs, whose physicochemical and electrochemical features possess prospective applications, particularly in multiferroics, electrodes for rechargeable lithium batteries, spintronics, optoelectronics, and superconductors [22]. The spinel  $\text{CuAl}_2\text{O}_4$  NPs are n-type semiconductor materials with a small bandgap energy of 1.8–2.3 eV that show high catalytic activity with thermal and mechanical stabilities. The high surface area and small particle size of  $\text{CuAl}_2\text{O}_4$  nanoparticles make them promising catalysts for large-scale catalytic applications [23]. The co-precipitation method is widely used because of its cost-effectiveness, scalability, excellent stoichiometric control, and readily controllable operating conditions [24]. However, there is limited literature available on the synthesis of  $\text{CuAl}_2\text{O}_4$  nanoparticles (NPs) using the co-precipitation method, highlighting the need for further investigation.

The green synthesis of nanoparticles has emerged as a sustainable and environmentally friendly alternative to conventional chemical synthesis methods. This sustainable approach exploits biological resources to generate the nanoparticles in a safe, harmless and eco-friendly manner [25]. This research work highlights the first-time use of *Jatropha curcas* leaf extracts for the fabrication of  $\text{CuAl}_2\text{O}_4$  NPs. *Jatropha curcas* is a drought-resistant shrub that belongs to the Euphorbiaceae family, which is recognized as an ornamental and bioenergy plant extensively found across Asia, Africa, and America [26-28]. The leaf extract is enriched with an essential phytoconstituents including alkaloids, flavonoids, tannins, saponins, steroids, glycosides, and phenolic compounds which having diverse biological activities like antimicrobial, antioxidant, anticancer, anti-inflammatory antifungal, and antibacterial properties as well as medicinal uses in the treatment of asthma, rheumatism, and pneumonia etc. [29-30]. Furthermore, the several parts of *J. curcas* plant including leaves, latex, and seed extracts, were utilized as reducing and stabilizing agents in the green synthesis of both monometallic and bimetallic oxide nano particles. The *J. Curcas* phytogenic extracts were used widely in the fabrication of ZnO [31], CuO[32], Ag[33],  $\text{TiO}_2$ [34],  $\text{CeO}_2$ [35],  $\text{MnO}_2$ [36], CuO-ZnO[37],  $\text{La}_2\text{O}_3/\text{ZnO}$ [38] nano particles.

To the best of our knowledge no any recent work yet published on photosynthesis of  $\text{CuAl}_2\text{O}_4$  NPs. Therefore, we reported the synthesis of  $\text{CuAl}_2\text{O}_4$  NPs via an eco-friendly green route using *Jatropha curcas* leaf extract as a reducing and stabilizing agent through the co-precipitation method. Moreover, structural and morphological properties were elucidated using spectroscopic and microscopic techniques such as XRD, FE-SEM, EDS and FT-IR Spectroscopy.

## 2. Experimental

### 2.1. Materials and Chemicals

The metal salt precursors; Copper nitrate trihydrate  $[\text{Cu}(\text{NO}_3)_2 \cdot 3\text{H}_2\text{O}]$  Aluminium sulphate octadeca hydrate  $[\text{Al}_2(\text{SO}_4)_3 \cdot 18\text{H}_2\text{O}]$  and solvents like Ammonium hydroxide, Ethanol, Acetone were used in the synthesis of  $\text{CuAl}_2\text{O}_4$  NPs. All the chemicals and reagents of analytical grade were purchased from Merck Pvt. Ltd. and Loba Chemie Pvt. Ltd., which were used without further purification. As the synthesized  $\text{CuAl}_2\text{O}_4$

NPs were characterized with different analytical techniques like XRD (Rigaku Mini flex 600), FE-SEM (Carl Zeiss Supra 55) and FT-IR spectra obtained using Shimadzu (KBr,  $\lambda_{\max}$  in  $\text{cm}^{-1}$ ).

## 2.2. Preparation of *Jatropha curcas* leaf extract

The fresh leaves of *J. curcas* were collected from areas along the roadside of Mendhepar village, Katol region, Maharashtra, India. The collected leaves were thoroughly cleaned several times with tap water, followed by deionized (DI) water and then dried in the shade for two days. The shade dried leaves were crushed into fine powder using mortar and pestle. 2.5 g of leaves powder was drenched in 100 ml of DI water while heating and stirring for 2 hrs. The brown-colored leaf extract was cooled down at room temperature and filtered using Whatman filter paper No. 41 [39].

## 2.3. Phytosynthesis of $\text{CuAl}_2\text{O}_4$ NPs

The  $\text{CuAl}_2\text{O}_4$  NPs were synthesized via co-precipitation method. In the typical synthesis procedure, 1 mM of  $\text{Al}_2(\text{SO}_4)_3 \cdot 18\text{H}_2\text{O}$  and 0.5 mM of  $\text{Cu}(\text{NO}_3)_2 \cdot 3\text{H}_2\text{O}$  were sonicated for 15 min in 50 mL DI water. The resultant suspensions were combined and agitated for an additional 15 minutes at  $80^\circ\text{C}$  to make a homogeneous solution. Subsequently, 50 mL of *J. curcas* leaf extract was added dropwise to the homogeneous precursor solutions under continuous stirring. The pH of the reaction mixture was adjusted to 9 using ammonium hydroxide solution. Furthermore, the resultant solution was stirred and heated for about 4 h up to the colour changes from dark green to sea foam green which primarily indicates the formation of  $\text{CuAl}_2\text{O}_4$  NPs. The precipitate was then centrifuged at

3000 rpm and washed repeatedly with DI water and ethanol. The collected product was further dried in a hot air oven at  $100^\circ\text{C}$  for 24 h, followed by calcination at  $600^\circ\text{C}$  for 4 h using muffle furnace.

## 3. Results and Discussion

### 3.1. X-ray diffraction (XRD) pattern analysis

The XRD technique used to determine the crystal structure, phase and purity of  $\text{CuAl}_2\text{O}_4$  NPs. The XRD pattern was recorded using  $\text{Cu K}\alpha$  radiation ( $\lambda=1.5406 \text{ \AA}$ ) over suitable  $2\theta$  range  $10^\circ$  to  $90^\circ$ . Fig.1 shows XRD pattern of the sample calcinated at  $600^\circ\text{C}$  exhibit broad diffraction peaks, indicating the formation of nanocrystalline  $\text{CuAl}_2\text{O}_4$  with low crystallinity. The diffraction peaks were observed at  $2\theta$  values of  $19.0^\circ$ ,  $31.3^\circ$ ,  $36.8^\circ$ ,  $44.8^\circ$ ,  $55.6^\circ$ ,  $59.4^\circ$ ,  $65.2^\circ$ ,  $74.0^\circ$ , and  $82.3^\circ$  are well indexed with crystal faces  $hkl$  reflection planes of (111), (220), (311), (400), (422), (511), (440), (620), and (444) respectively. From the above values (311) shows the highest intensity peak which is typical feature of spinel-type oxides. This study revealed a cubic phase with the spinel structure of the  $\text{CuAl}_2\text{O}_4$  NPs match well with the standard JCPDS No. 33-0448. The broad peak around  $35\text{--}36^\circ$  overlaps with the characteristic CuO reflection, however, the absence of the prominent CuO peaks at approximately  $38.7^\circ$ ,  $48.7^\circ$  and  $53.5^\circ$  suggest that any residual CuO is negligible. The broad nature of the diffraction peaks is attributed to the relatively low calcination temperature [40-41]. The average crystallite size of the synthesized  $\text{CuAl}_2\text{O}_4$  nanoparticles was estimated using the Debye-Scherrer equation and found to be 55 nm.

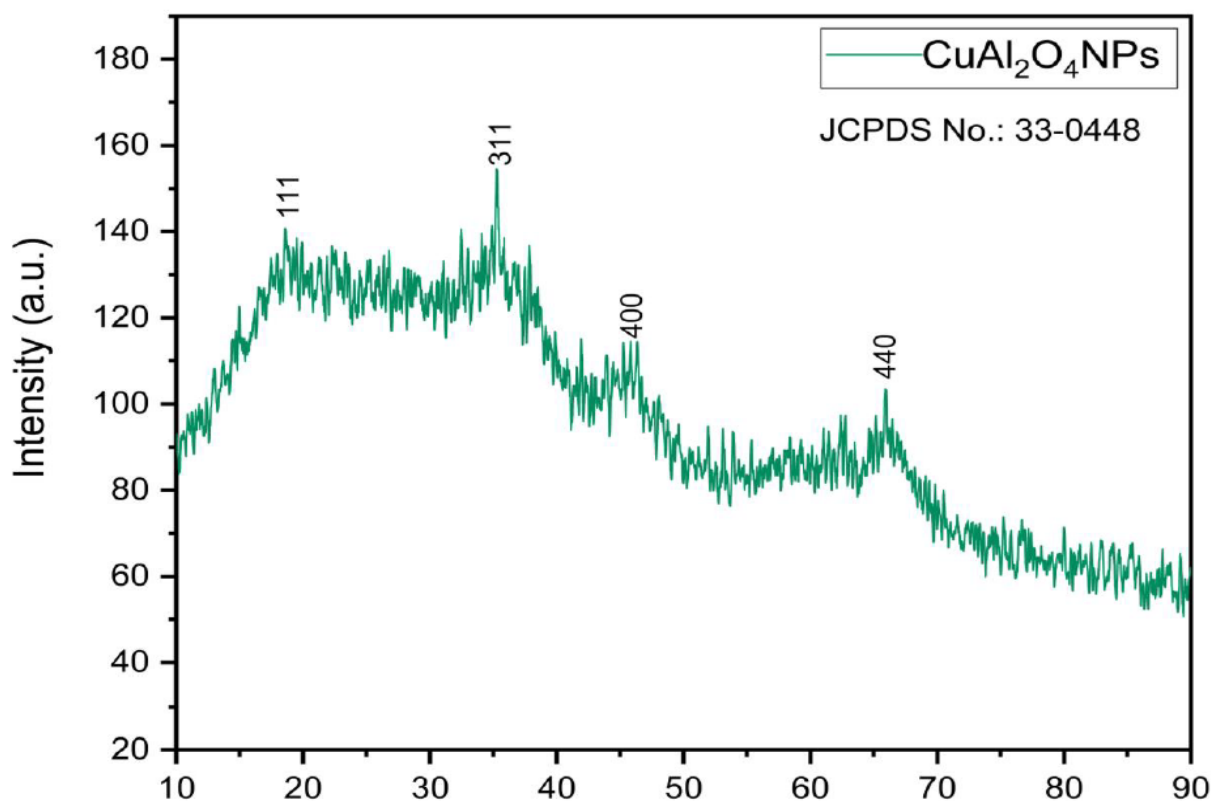


**Fig.1:X-Ray diffraction patterns of  $\text{CuAl}_2\text{O}_4$  NPs.**

### 3.2. FE-SEM and EDS with elemental mapping analysis

FE-SEM combined with EDS was utilized to examine the surface morphology, elemental composition, and purity of the synthesized  $\text{CuAl}_2\text{O}_4$  NPs. The FE-SEM images (Fig. 2) reveal densely agglomerated flake like clusters composed of densely packed nanosized primary particles. Such agglomeration is commonly observed in spinel oxide nanoparticles because of their elevated surface energy and robust interparticle interactions among the metal oxide nanoparticles [42-43]. At low magnification, the particles appear as large aggregates randomly distributed over the surface. Higher magnification images show that these aggregates consist of densely packed nanosized primary particles with rough surfaces. The observed agglomeration can be attributed to the high surface energy of  $\text{CuAl}_2\text{O}_4$  nanoparticles and the interaction among particles during drying and calcination. In addition, the phyto chemicals present in the plant extract used during green synthesis may influence the nucleation and growth processes, leading to the formation of flake-like aggregated structures. The elemental composition of the synthesized  $\text{CuAl}_2\text{O}_4$

nanoparticles was investigated by energy-dispersive X-ray spectroscopy (EDS), and the corresponding elemental distribution was examined by elemental mapping, as presented in Fig.3(a-b). The EDS spectrum exhibits characteristic peaks corresponding exclusively to oxygen (O), aluminium (Al), and copper (Cu), confirming the successful formation of  $\text{CuAl}_2\text{O}_4$  nanoparticles. No additional elemental peaks were detected, indicating the absence of detectable foreign elemental impurities. The quantitative EDS analysis reveals atomic percentages of 65.0% O, 28.8% Al, and 6.2% Cu. The higher oxygen content is expected because oxygen atoms are present in greater numbers in the oxide lattice. The elemental mapping images demonstrate a uniform distribution of Cu, Al, and O throughout the analyzed region without obvious elemental segregation, suggesting homogeneous incorporation of the constituent elements within the oxide matrix. However, XRD analysis revealed a weak diffraction peak corresponding to the secondary monoclinic CuO phase, indicating the presence of a minor crystalline impurity.

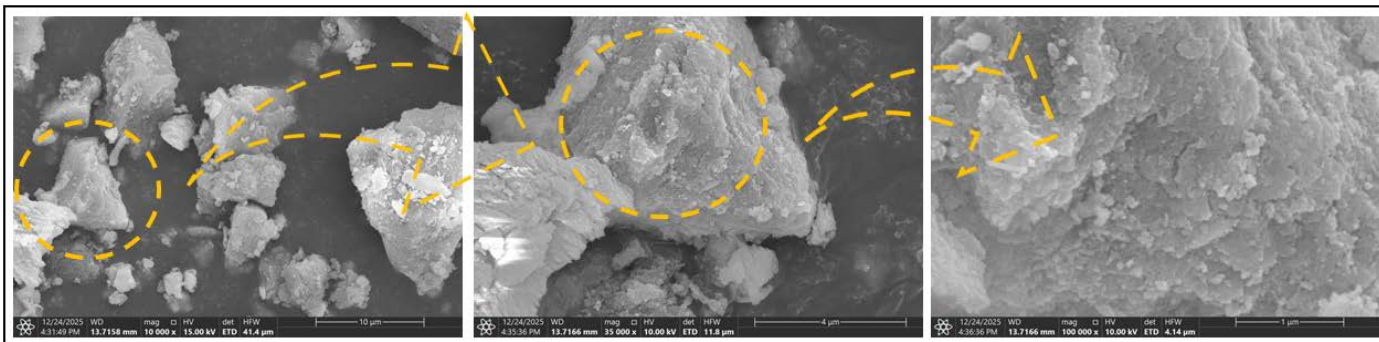


Fig.2:FE-SEM Micrographs of  $\text{CuAl}_2\text{O}_4$  NPs

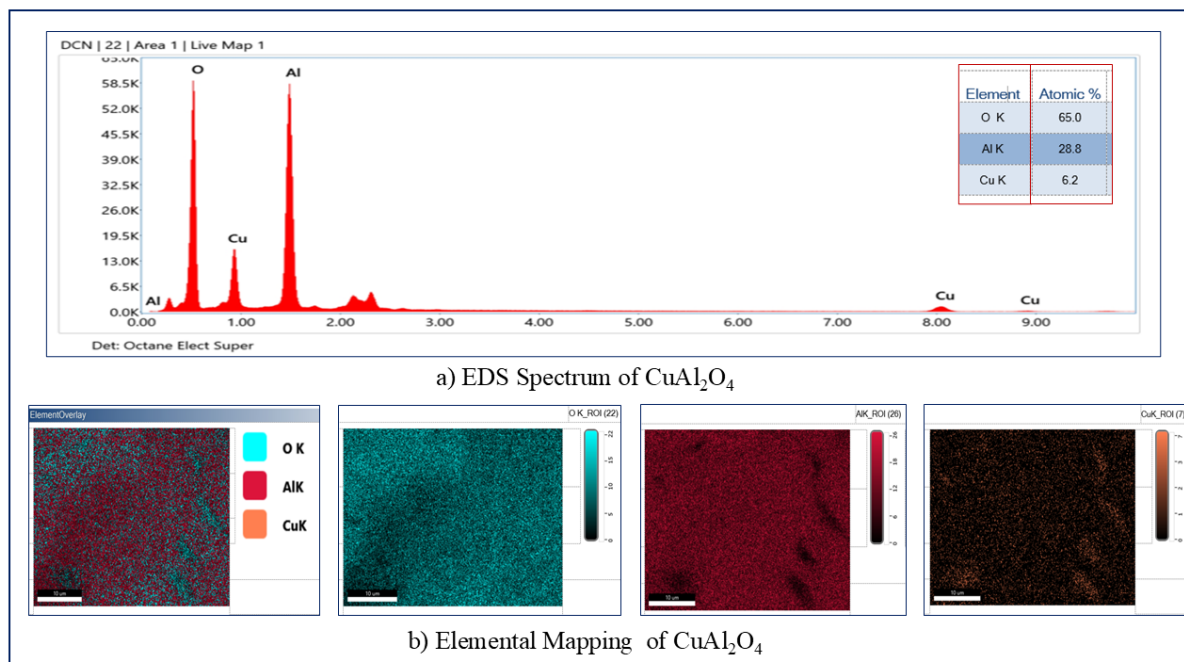


Fig.3: EDS Spectrum and Elemental Mapping of  $\text{CuAl}_2\text{O}_4$

### 3.3. FT-IR analysis

The FT-IR analysis of  $\text{CuAl}_2\text{O}_4$  NPs confirmed the presence of the functional groups present in the *Jatropha curcas* leaf powder which was utilized as essential bio reductants and stabilizers for the green synthesis of the  $\text{CuAl}_2\text{O}_4$  NPs as shown in Fig 4. The recorded FT-IR spectrum of leaf powder exhibits the distinct absorption peak due to carbonyl, hydroxyl, aromatic, and ether functional groups. After the synthesis of  $\text{CuAl}_2\text{O}_4$  NPs, the several notable changes were observed in the FT-IR spectrum. The diminished intensities of absorptions bands which reveals the utilization of biomolecules present in the leaf extract during the typical NPs synthesis. A broad absorption band centered at  $3363.03 \text{ cm}^{-1}$  in the leaf powder spectrum is attributed to the stretching vibrations of hydroxyl groups present in phenolic compounds, flavonoids, alcohols, and adsorbed water molecules. After nanoparticle synthesis, this band shifted to  $3442.12 \text{ cm}^{-1}$  and became broader, suggesting the interaction of

hydroxyl-containing biomolecules with the surface of  $\text{CuAl}_2\text{O}_4$  nanoparticles. This shift indicates that these phytochemicals participated in the reduction of metal ions and subsequently acted as stabilizing agents. A weak absorption band observed at  $2932 \text{ cm}^{-1}$  in the leaf powder corresponds to the asymmetric stretching vibrations of aliphatic C-H groups originating from lipids, carbohydrates, and other organic constituents. The reduced intensity or disappearance of this band in the nanoparticle spectrum indicates the consumption or rearrangement of these organic molecules during nanoparticle formation. The prominent band at  $1100 \text{ cm}^{-1}$  observed in the leaf powder is assigned to C-O, C-O-C, or C-N stretching vibrations associated with carbohydrates, alcohols, ethers, and glycosidic compounds. After nanoparticle synthesis, this band shifted to  $1124 \text{ cm}^{-1}$ , indicating the involvement of oxygen-containing functional groups in the complexation and stabilization of  $\text{Cu}^{2+}$  and  $\text{Al}^{3+}$  ions during nanoparticle formation. The most

significant evidence for successful  $\text{CuAl}_2\text{O}_4$  nanoparticle formation is the appearance of new absorption bands at  $615\text{ cm}^{-1}$  and  $519\text{ cm}^{-1}$ . These low-frequency bands are absent in the leaf powder spectrum and are characteristic of metal–oxygen (M–O) stretching vibrations within the spinel lattice. The band

around  $615\text{ cm}^{-1}$  is generally assigned to the stretching vibrations of Al–O bonds at tetrahedral sites, whereas the band near  $519\text{ cm}^{-1}$  corresponds to Cu–O vibrations associated with octahedral coordination. These characteristic vibrations confirm the formation of the spinel  $\text{CuAl}_2\text{O}_4$  crystal structure[44].

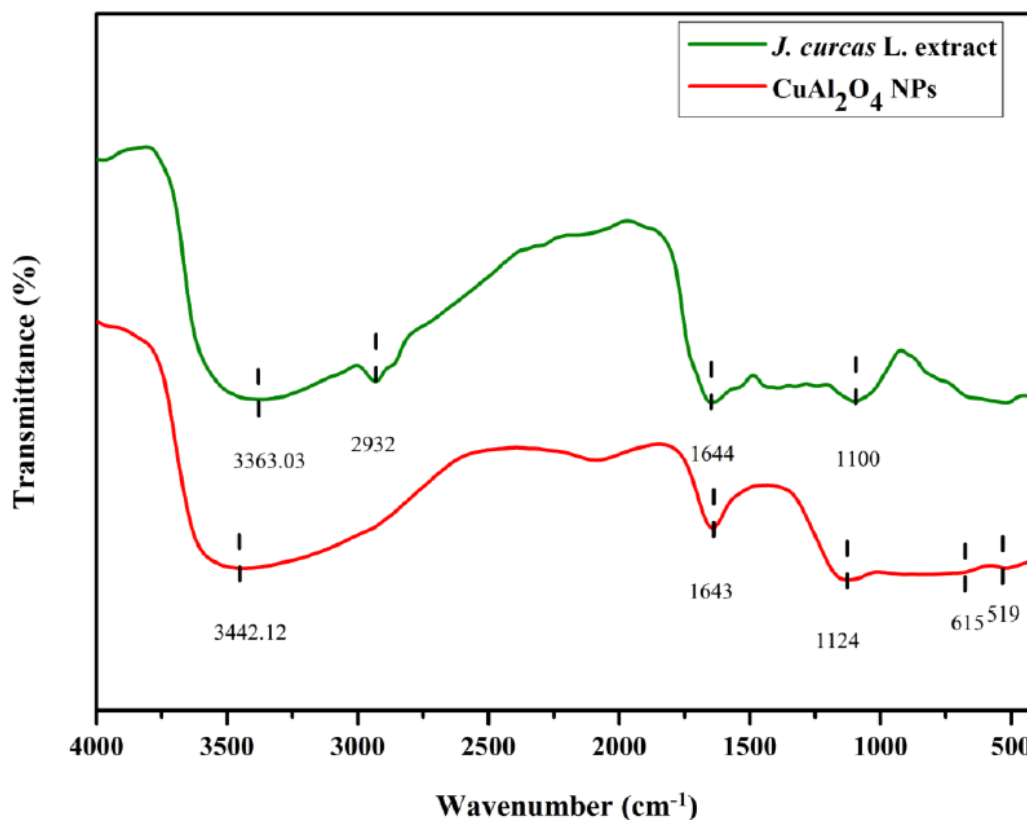


Fig.4:FT-IR Analysis of *J. curcas* L. Extract and  $\text{CuAl}_2\text{O}_4$  NPs

#### 4. Conclusion and Future Perspectives

The present study highlights the effectiveness of *Jatropha curcas* leaf extract as a sustainable and eco-friendly synthesis of  $\text{CuAl}_2\text{O}_4$  NPs instead of traditional methods. In the given synthetic method, the  $\text{CuAl}_2\text{O}_4$  NPs were fabricated via co-precipitation method using *J. curcas* leaf extract as reducing and stabilizing agent. The successful synthesis of the cubic spinel  $\text{CuAl}_2\text{O}_4$  NP was confirmed through comprehensive characterization using XRD, FT-IR, FE-SEM, and EDS analyses. These results verified the low crystalline nature, morphology, elemental composition, and surface functional groups of the synthesized  $\text{CuAl}_2\text{O}_4$  NPs. The FE-SEM result proven the formation of agglomerated  $\text{CuAl}_2\text{O}_4$  NPs with flake like nanostructures with rough surface morphology. EDS and elemental mapping result confirmed

the composition and purity of prepared  $\text{CuAl}_2\text{O}_4$  NPs with uniform distribution of Cu, Al, and O in the nanomaterial. FT-IR analysis suggested the involvement of phytochemical constituents of plant extract in the mechanism of reduction, capping, and stabilization, while distinct metal-oxygen vibrational band further confirmed the formation of  $\text{CuAl}_2\text{O}_4$  nanoparticles. This study demonstrates that the proposed green synthesis approach is an efficient, environmentally friendly, and cost-effective method for producing  $\text{CuAl}_2\text{O}_4$  NPs with desirable structural and functional characteristics. Future investigations should focus on evaluating their catalytical, antimicrobial, antioxidant, cytotoxicity, and biocompatibility properties to establish their suitability for biomedical applications. Furthermore, the developed green synthesis

strategy may be extended to other mixed-metal oxide systems, facilitating the development of cost-effective and sustainable nanomaterials for advanced technological applications.

### References:

- Potbhare, A. K., Chauke, P. B., Zahra, S., Sonkusare, V., Bagade, R., Ummekar, M., & Chaudhary, R. G. (2019). Microwave-mediated fabrication of mesoporous Bi-doped  $\text{CuAl}_2\text{O}_4$  nanocomposites for antioxidant and antibacterial performances. *Materials Today: Proceedings*, 15, 454-463.
- Zhao, Q., Yan, Z., Chen, C., & Chen, J. (2017). Spinels: controlled preparation, oxygen reduction/evolution reaction application, and beyond. *Chemical reviews*, 117(15), 10121-10211.
- Menon, S. G., Kulkarni, S. D., Choudhari, K. S., & C, S. (2016). Diffusion-controlled growth of  $\text{CuAl}_2\text{O}_4$  nano particles: effect of sintering and photo degradation of methyl orange. *Journal of Experimental Nano science*, 11(15), 1227-1241.
- Khalifeh, R., Karimi, M., Rajabzadeh, M., Hafizi, A., & Nogorani, F. S. (2020). Synthesis and morphology control of nano  $\text{CuAl}_2\text{O}_4$  hollow spheres and their application as an efficient and sustainable catalyst for  $\text{CO}_2$  fixation. *Journal of  $\text{CO}_2$  Utilization*, 41, 101233.
- Han, M., Wang, Z., Xu, Y., Wu, R., Jiao, S., Chen, Y., & Feng, S. (2018). Physical properties of  $\text{MgAl}_2\text{O}_4$ ,  $\text{CoAl}_2\text{O}_4$ ,  $\text{NiAl}_2\text{O}_4$ ,  $\text{CuAl}_2\text{O}_4$ , and  $\text{ZnAl}_2\text{O}_4$  spinels synthesized by a solution combustion method. *Materials Chemistry and Physics*, 215, 251-258.
- Naderi, M., Shamirian, A., & Edrisi, M. (2011). Synthesis, characterization and photocatalytic properties of nanoparticles  $\text{CuAl}_2\text{O}_4$  by Pechini method using Taguchi statistical design. *Journal of sol-gel science and technology*, 58(2), 557-563.
- Tran, A. T., Tran, V. T., Nguyet, N. T. M., Luong, A. T. Q., Le, T. V., & Phuc, N. H. H. (2023). Solid-state reaction synthesis of  $\text{MgAl}_2\text{O}_4$  spinel from  $\text{MgO-Al}_2\text{O}_3$  composite particles prepared via electrostatic adsorption. *ACS omega*, 8(39), 36253-36260.
- Eslami, A., Lachini, S. A., Shaterian, M., Karami, M., & Enhessari, M. (2024). Sol-gel synthesis, characterization, and electrochemical evaluation of magnesium aluminate spinel nanoparticles for high-capacity hydrogen storage. *Journal of Sol-Gel Science and Technology*, 109(1), 215-225.
- Baruah, B., Bhattacharyya, S., & Sarkar, R. (2023). Synthesis of magnesium aluminate spinel—An overview. *International Journal of Applied Ceramic Technology*, 20(3), 1331-1349.
- Jagadeeshwaran, C., Madhan, K., & Murugaraj, R. (2018). Size effect and order-disorder phase transition in  $\text{MgAl}_2\text{O}_4$ : Synthesized by co-precipitation method. *Journal of Materials Science: Materials in Electronics*, 29(22), 18923-18934.
- Potbhare, A. K., Yerpude, S., Daddemal-Chaudhary, A. R., Lambat, A., Mondal, A., Dadure, K. M., & Chaudhary, R. G. (2024). Catharanthus roseus-mediated  $\text{CuAl}_2\text{O}_4$  nanocomposites for evaluation of killing kinetics. *Chemosphere*, 359, 142369.
- Staszak, W., Zawadzki, M., & Okal, J. (2010). Solvothermal synthesis and characterization of nanosized zinc aluminate spinel used in iso-butane combustion. *Journal of Alloys and compounds*, 492(1-2), 500-507.
- Chen, Z. Z., Shi, E. W., Li, W. J., Zheng, Y. Q., Zhuang, J. Y., Xiao, B., & Tang, L. A. (2004). Preparation of nanosized cobalt aluminate powders by a hydrothermal method. *Materials Science and Engineering: B*, 107(2), 217-223.
- Queiroz, R. M., Coelho, T. L., Queiroz, I. M., Pires, L. H., Santos, I. M., Zamian, J. R., & da Costa, C. E. (2016). Structural and thermal characterization of  $\text{Ni}_x\text{Zn}_{1-x}\text{Al}_2\text{O}_4$  synthesized by the polymeric precursor method. *Journal of Thermal Analysis and Calorimetry*, 124(2), 1023-1028.
- Moheb, A., Abedini, K. S., & Moradi, D. S. (2020). Effect of Solvents on the Synthesis of  $\text{SrAl}_2\text{O}_4$  Nanoparticles by Reverse Micelle Process.
- Lv, W., Liu, B., Qiu, Q., Wang, F., Luo, Z., Zhang, P., & Wei, S. (2009). Synthesis, characterization and photocatalytic properties of spinel  $\text{CuAl}_2\text{O}_4$  nanoparticles by a sonochemical method. *Journal of alloys and compounds*, 479(1-2), 480-483.
- Ragupathi, C., Vijaya, J. J., Kennedy, L. J., & Bououdina, M. (2014). Combustion synthesis, structure, magnetic and optical

- properties of cobalt aluminate spinel nanocrystals. *Ceramics International*, 40(8), 13067-13074.
18. Mohamed, S. A., Mekkey, S. D., Othman, A. M., & El-Sakhawy, M. (2024). Novel antimicrobial biodegradable composite films as packaging materials based on shellac/chitosan, and ZnAl<sub>2</sub>O<sub>4</sub> or CuAl<sub>2</sub>O<sub>4</sub> spinel nanoparticles. *Scientific Reports*, 14(1), 27824.
  19. Hosseini, S. A. (2017). Synthesis of CuAl<sub>2</sub>O<sub>4</sub> nanostructures with the aid of different amino acids as a fuel and its photocatalyst application. *Journal of Materials Science: Materials in Electronics*, 28(4), 3762-3767.
  20. Gholami, A., & Maddahfar, M. (2016). Synthesis and characterization of novel samarium-doped CuAl<sub>2</sub>O<sub>4</sub> and its photocatalytic performance through the modified sol-gel method. *Journal of Materials Science: Materials in Electronics*, 27(4), 3341-3346.
  21. Edrisi, M., Tajik, S., & Soleymani, M. (2013). Synthesis of CuAl<sub>2</sub>O<sub>4</sub> nanoparticles by mixed chelates thermolysis and homogeneous precipitation using solubility difference reactions; Taguchi optimization and photocatalytic application. *Journal of Materials Science: Materials in Electronics*, 24(10), 3914-3920.
  22. Andal, V., Buvaneswari, G., & Lakshmi, R. (2021). Synthesis of CuAl<sub>2</sub>O<sub>4</sub> nanoparticle and its conversion to CuO nanorods. *Journal of Nanomaterials*, 2021(1), 8082522.
  23. Lahmar, H., Douafer, S., Laouici, R., Hamdi, M., Souici, A., Trari, M., & Benamira, M. (2024). Synthesis and characterization of CuAl<sub>2</sub>O<sub>4</sub> nanoparticles: Application for the removal of Eriochrome Black T under solar light irradiation. *Inorganic Chemistry Communications*, 163, 112316.
  24. Li, Z., Sun, Y., Ge, S., Zhu, F., Yin, F., Gu, L., & Volinsky, A. A. (2023). An overview of synthesis and structural regulation of magnetic nanomaterials prepared by chemical coprecipitation. *Metals*, 13(1), 152.
  25. Rakshit, S., Jana, P. C., & Kamilya, T. (2023). Green synthesis of copper nanoparticles by using plant extracts and their biomedical applications—an extensive review. *Current Nanomaterials*, 8(2), 110-125.
  26. Arekemase, M. O., Kayode, R. M. O., & Ajiboye, A. E. (2011). Antimicrobial activity and phytochemical analysis of *Jatropha curcas* plant against some selected microorganisms. *International Journal of Biology*, 3(3), 52-59.
  27. Najda, A., Almehemdi, A. F., & Zabar, A. F. (2013). Chemical composition and nutritional value of *Jatropha curcas* L.) leaves. *Journal of Genetic and Environment Conservation*, 1(3), 222-227.
  28. Rahu, M. I., Naqvi, S. H. A., Memon, N. H., Idrees, M., Kandhro, F., Pathan, N. L., ... & Bhutto, M. A. (2021). Determination of antimicrobial and phytochemical compounds of *Jatropha curcas* plant. *Saudi journal of biological sciences*, 28(5), 2867-2876.
  29. Sharma, A. K., Gangwar, M., Kumar, D., Nath, G., Sinha, A. S. K., & Tripathi, Y. B. (2016). Phytochemical characterization, antimicrobial activity and reducing potential of seed oil, latex, machine oil and presscake of *Jatropha curcas*. *Avicenna journal of phytomedicine*, 6(4), 366.
  30. Rahu, M. I., Naqvi, S. H. A., Memon, N. H., Idrees, M., Kandhro, F., Pathan, N. L., & Bhutto, M. A. (2021). Determination of antimicrobial and phytochemical compounds of *Jatropha curcas* plant. *Saudi journal of biological sciences*, 28(5), 2867-2876.
  31. Sharma, Y., Anand, V., Kumar, R., Kumar, A., & Heera, P. (2025). Green synthesized ZnO nanoparticles using *Jatropha curcas* latex for antibacterial applications. *Next Materials*, 8, 100869.
  32. Al Mazroui, M. M. S., Devi, G., Al Abdali, A. M. A. H., & Al Alawi, S. M. K. (2025). Bio Synthesis of Copper oxide Nanoparticles from *Jatropha Curcas* Leaf Extract and Their Antibacterial Activity Study. In *BIO Web of Conferences* (Vol. 160, p. 02002). EDP Sciences.
  33. Chauhan, N., Tyagi, A. K., Kumar, P., & Malik, A. (2016). Antibacterial potential of *Jatropha curcas* synthesized silver nanoparticles against food borne pathogens. *Frontiers in microbiology*, 7, 1748.
  34. Goutam, S. P., Saxena, G., Singh, V., Yadav, A. K., Bharagava, R. N., & Thapa, K. B. (2018). Green synthesis of TiO<sub>2</sub> nanoparticles using leaf extract of *Jatropha curcas* L. for photocatalytic degradation of

- tannery wastewater. *Chemical Engineering Journal*, 336, 386-396.
35. Magudieshwaran, R., Ishii, J., Raja, K. C. N., Terashima, C., Venkatachalam, R., Fujishima, A., & Pitchaimuthu, S. (2019). Green and chemical synthesized CeO<sub>2</sub> nanoparticles for photocatalytic indoor air pollutant degradation. *Materials Letters*, 239, 40-44.
36. Byeon, H., Suvain, K. K., Singh, P. K., Babu, L. G., & MC, P. (2026). Effective removal and inactivation of toxic pollutants from biological staining through the novel *Jatropha curcas* abetted MnO<sub>2</sub> nanoparticles. *Surfaces and Interfaces*, 109827.
37. Sharma, Y., Anand, V., Dhiman, V., & Heera, P. (2025). Biogenic CuO-ZnO nanocomposites synthesized from *Jatropha curcas* for methylene blue dye degradation. *JCIS Open*, 100146.
38. Sharma, A., Singh, S., Sharma, K., Thakur, K., Choudhary, K., Patial, A., & Dhiman, V. (2025). Green approach to La<sub>2</sub>O<sub>3</sub>/ZnO nanocomposites synthesis via *Jatropha curcas* latex: Implications in photocatalysis. *JCIS Open*, 18, 100140.
39. Shingda, S. R., Fuke, R., Alone, H. M., Ganorkar, K. S., Chaudhary, R. G., Mondal, S., & Gandhare, N. V. (2026). Sustainable biosynthesis of microporous platinum-doped NiZn<sub>2</sub>O<sub>4</sub> nanocomposites as an efficient catalyst for the synthesis of pyrano [2, 3-c] pyrazole and its derivatives. *Research on Chemical Intermediates*, 1-21.
40. Zhang, J., Shao, C., Li, X., Xin, J., Yang, S., & Liu, Y. (2018). Electrospun CuAl<sub>2</sub>O<sub>4</sub> hollow nanofibers as visible light photocatalyst with enhanced activity and excellent stability under acid and alkali conditions. *CrystEngComm*, 20(3), 312-322.
41. Gao, F., Zhang, R., Liu, J., Gao, Z., & Huang, W. (2024). An investigation into the impact of CuAl<sub>2</sub>O<sub>4</sub> hydrophobization on catalyst structure and performance for syngas conversion. *Applied Surface Science*, 661, 160072.
42. Singh, P., Kim, Y. J., Zhang, D., & Yang, D. C. (2016). Biological synthesis of nanoparticles from plants and microorganisms. *Trends in biotechnology*, 34(7), 588-599.
43. Wu, L., Wu, Y., & Lü, Y. (2006). Self-assembly of small ZnO nanoparticles toward flake-like single crystals. *Materials Research Bulletin*, 41(1), 128-133.
44. Umezulora, B. I., Okoye, E. L., Uba, B. O., & Anaebonmam, E. C. (2026). Phytochemical Profiling of Aqueous, Methanol and Hexane Leaf Extracts of *Jatropha curcas* using Chromatographic and Spectral Finger-Printings. *Journal of Phytochemistry, Ethnobotany and Traditional Medicine Systems*, 2(1), 35-44.